

Split and Expand: An inference-time improvement for Weakly Supervised Cell Instance Segmentation

Lin Geng Foo¹, Rui En Ho¹, Jiamei Sun¹, and Alexander Binder^{2,3}

¹ Singapore University of Technology and Design, Singapore

² University of Oslo, Norway

³ Singapore Institute of Technology, Singapore

Abstract. We consider the problem of segmenting cell nuclei instances from Hematoxylin and Eosin (H&E) stains with weak supervision. While most recent works focus on improving the segmentation quality, this is usually insufficient for instance segmentation of cell instances clumped together or with a small size. In this work, we propose a two-step post-processing procedure, *Split* and *Expand*, that directly improves the conversion of segmentation maps to instances. In the *Split* step, we split clumps of cells from the segmentation map into individual cell instances with the guidance of cell-center predictions through Gaussian Mixture Model clustering. In the *Expand* step, we find missing small cells using the cell-center predictions (which tend to capture small cells more consistently as they are trained using reliable point annotations), and utilize Layer-wise Relevance Propagation (LRP) explanation results to expand those cell-center predictions into cell instances. Our *Split* and *Expand* post-processing procedure is *training-free* and is executed at inference-time only. To further improve the performance of our method, a feature re-weighting loss based on LRP is proposed. We test our procedure on the MoNuSeg and TNBC datasets and show that our proposed method provides statistically significant improvements on object-level metrics. Our code will be made available.

Keywords: Cell Instance Segmentation · Weakly Supervised · Computational Pathology

1 Introduction

Instance segmentation is crucial in many biomedical applications, such as phenotyping [7], cell-tracking [27] and computer-aided cancer diagnosis [9,6]. Deep learning models can potentially be deployed to improve instance segmentation quality [12] and increase the reliability of these applications, but require large amounts of high quality annotated data. Moreover, getting fully annotated datasets of medical images is *expensive* [20,5,21], e.g. for H&E stains, many pixels need to be carefully annotated for each individual cell. It is thus costly for qualified medical experts to annotate large databases, yet alternatives such as

cloud annotation are less reliable. Conversely, it is much easier to obtain *dot-annotated* datasets (e.g. only one pixel in each cell needs to be annotated), which is the primary motivating factor behind weakly supervised segmentation.

The prevailing approach for weakly supervised (dot-annotated) cell segmentation problem consists of generating coarse labels using various methods (e.g. Voronoi partitioning and clustering), and training the segmentation model using these labels [20,10,8,26,28]. While this approach works rather well for segmenting foreground pixels from the background, the conversion from the output segmentation map to the instance segmentation one is still coarsely done using basic morphological operations. In many cases, boundaries between cells are not well handled by these morphological operations, leading to clumps of cells being mistakenly identified as a single instance. Additionally, we also observe that small cells are often missed in the output segmentation map, which is likely due to the errors in the coarse labels (as noted in [20,10,8]), that might disproportionately affect the smaller cells more. Both of these are potentially critical issues, especially when the number of cells detected is a primary concern, e.g cell counting.

In our work, we tackle the aforementioned problems with a two-step post-processing procedure at inference time. To tackle the *mishandling of boundaries leading to clumps of cells identified as instances*, we introduce a *Split* step that performs splitting of clumps of cells when multiple cell centers have been identified within a clump. We split the clumps into instances through a Gaussian Mixture Model clustering, while taking into account the confidence of cell center prediction maps, such that pixels with lower prediction values within the clumps are likelier to be the boundaries between cells. To tackle the *problem of missing small cells*, we introduce an *Expand* step where our model predicts the locations of cell centers, and performs the “expansion” of some predicted cell centers (those not identified in the segmentation map) into entire cell instances. Crucially, the supervision for the cell-center (CC) prediction task comes from the *reliable dot annotations* (and not the processed coarse labels), which makes these CC predictions more likely to be accurate than the segmentation map. We adopt an explanation method, LRP, to identify entire small cells from predicted cell centers. Intuitively, each point predicted by our model to be a cell center is predicted as such due to an identified *cell instance around that point*, and *LRP produces a heatmap that precisely highlights that cell instance* to explain the cell center prediction. LRP is capable of identifying the inputs that are related to the predictions and provides high-quality explanations and visualizations in many evaluation studies [19,22,3,16].

To accomplish the post-processing procedure above, we require the prediction of CCs, thus we add another head to our segmentation model that does CC prediction, and simultaneously train both heads (segmentation and CC-prediction) during training. However, the CC-prediction task is challenging as CCs are sparse compared to the background. To get better accuracy on the CC output head, we propose a feature re-weighting (FRW) loss based on explanation methods inspired by [25]. This loss re-weights features using explanation scores, such that

features that contribute more towards the rare class (positive CC prediction) are up-weighted, leading to better training on the imbalanced dataset.

To summarize, our contributions are:

1. We propose a novel post-processing procedure, *Split and Expand*, for cell instance segmentation. *Split and Expand* is training-free and model-agnostic, and improves cell instance segmentation by resolving the clumps of cells and missing small cells in the segmentation map. To our best knowledge, we are the first to segment cell instances with the guidance of explanation results.

2. To overcome the label imbalance when training the cell-center output head, we propose a feature re-weighting loss that leads to further improvements.

3. Experiments on MoNuSeg [15] and TNBC [17] datasets show that our proposed methods provide statistically significant improvements over the baseline.

2 Related Work

Weakly supervised cell segmentation is the task where a cell segmentation model is trained using weak supervision (usually dot-annotated data), and has been receiving more attention recently due to its practical utility. Notably, [20] pre-processed point labels into Voronoi cells and clusters based on color and used them as coarse labels, [29] proposed to train an edge network, [8] proposed a repel encoding loss, [28] proposed to use coarse distance labels and [18] proposed an adversarial training method. Recently, [26,10] further proposed new methods involving self-training. Throughout these works, the instance segmentation output is obtained by applying morphological operations on the output segmentation map. Differently, our Split and Expand method further refines cell instances by *splitting up clumps* into smaller instances, *finding small instances* through CC-prediction (trained with reliable dot annotations) and *expanding them* using explanation results from LRP. To the best of our knowledge, our method is the first to tackle these issues. We further note that our work is complementary to the others proposed above (which generally focus on the training stage), and can be *easily added onto their methods*.

LRP is one of the explanation methods that aim at de-mystifying the black box of deep neural networks (DNN) and interpreting the model decisions [4]. The explanation results reflect the contribution of a neuron to the model decision, which is helpful for understanding the models [16,1]. Recently, several works studied the applications of explanation results [11,25] in other domains. To our best knowledge, we are the first work to utilize explanation methods to guide cell instance segmentation, whether it be our Expand step, or the FRW loss.

3 Method

3.1 Data pre-processing

We pre-process our dot-annotated labels into various other forms to train both the segmentation head and the CC-prediction head.

To train the CC-prediction head, we require Enlarged Point labels GT_P which are obtained by expanding each point label into a 3×3 square. GT_P is reliable, and helps provide stronger supervision for the model than point labels.

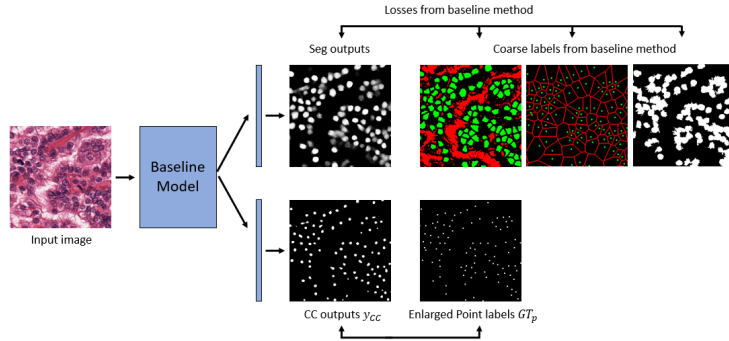


Fig. 1. An overview of our training method, network outputs, labels and losses. For visualization purposes, we show the Cluster, Voronoi and Superpixel coarse labels. We emphasize that our method can be *easily applied onto most existing segmentation baseline methods*, by simply adding a CC output head to the baseline model.

To train the segmentation head, we generate the coarse labels that our baseline model needs, e.g. when using [20] as the baseline, we need Cluster and Voronoi labels. We highlight that our post-processing method is model-agnostic, and can work effectively on different baselines and coarse labels.

3.2 Cell-center predictions and feature re-weighting loss

A summary of our proposed network and losses can be seen in Figure 1. As our method focuses on post-processing, we can adopt any baseline model, loss, or labels for the segmentation output. Moreover, we adapt the model to also generate an extra CC output y_{CC} from its features. The CC output is trained using pixel-wise cross entropy loss with respect to the Enlarged Point labels GT_P . Crucially, GT_P is reliable as it is annotated by experts, and thus the CC prediction tends to perform better than segmentation (especially on smaller cells where the coarse labels might contain more errors). Moreover, we note that there is a large label imbalance of CC pixels compared to background pixels in GT_P , that might affect performance. To further improve the training of the CC output y_{CC} under this label imbalance, we additionally propose a FRW loss L_{FRW} with respect to the Enlarged Point labels GT_P , which we describe next.

A core part of our FRW loss is LRP, which is capable of explaining the decisions of various DNNs [4,2,23,13]. It assigns an explanation score to every neuron that reflects supporting (positive scores) or opposing (negative scores) contribution to the predictions [16]. Furthermore, compared to other gradient-based explanation methods, LRP explanation scores reflect more of the related features that are used by the model to make decisions, which has been evaluated

in [19,22,3]. Thus, we apply the LRP explanations to design the feature re-weighting loss, L_{FRW} . In other domains, such explanation-guided losses have been known to perform well on small sample sizes or imbalanced datasets in other domains [25,24], and the latter presents itself in our CC prediction task.

Let \mathbf{f}_l denote the feature map of layer l in our model. We first perform a forward pass through the model to generate an original prediction y_{CC} . We then explain the generated prediction with LRP and obtain the explanation scores of the feature map $R(\mathbf{f}_l)$. We refer to the $LRP_{\alpha 1}$ rule to calculate $R(\mathbf{f}_l)$, as suggested in [14]. The re-weighted feature $\hat{\mathbf{f}}_l$ is calculated as follows:

$$w(\mathbf{f}_l) = l_{norm}(R(\mathbf{f}_l)) + 1, \hat{\mathbf{f}}_l = w(\mathbf{f}_l) \odot \mathbf{f}_l \quad (1)$$

where l_{norm} is a normalization layer where we divide using the maximum absolute value, $w(\mathbf{f}_l)$ is the generated weight for feature map \mathbf{f}_l , \odot is the Hadamard product operation, and $\hat{\mathbf{f}}_l$ is the re-weighted feature. The re-weighted feature $\hat{\mathbf{f}}_l$ is then fed forward to obtain a new output \hat{y}_{CC} , and the cross entropy loss is calculated with respect to the Enlarged Point labels.

With the re-weighting operation, we have $w(\mathbf{f}_l) > 1$ for the features with positive LRP explanation scores (indicating support) and $w(\mathbf{f}_l) < 1$ for those with negative LRP explanation scores (indicating opposition) [16,25]. Thus, the re-weighted features up-scale the related parts and are tuned more with L_{FRW} .

Our final loss for the CC output head is as follows, where α_P, α_{FRW} represent the weights of the Point and FRW losses:

$$Loss_{CC} = L_P + L_{FRW} = \alpha_P CE(y_{CC}, GT_P) + \alpha_{FRW} CE(\hat{y}_{CC}, GT_P) \quad (2)$$

3.3 Post-processing: Split and Expand

At test time, we obtain our Segmentation output and perform morphological operations (remove small objects, fill holes) to get an instance segmentation map. We then use our CC output to conduct our two-step post-processing (Split and Expand) on the instance segmentation map. The Split step helps to split clumps of cells into instances, while the Expand step helps to materialize the small cells (whose CCs have been predicted), which are often missed in the segmentation map. We emphasize that we *do not train on the post-processing task explicitly*. An overview of this process can be seen in Figure 2.

The first step is the *Split* step, which is a short form for Instance-Splitting. We first condense all blobs of CC outputs into single CC points by applying the same morphological operations and taking the center of each blob instance. Then, we find instances in our instance segmentation map that cover two or more CC points. Intuitively, these identified instances are *clumps* that contain two or more cells in close proximity, e.g. a clump containing k CCs is likely to contain k cell instances. Next, we perform weighted clustering based on CC predictions within these clumps to split them into k smaller instances, where *each cell instance is a cluster of pixels*. As most cells have a roughly ellipsoidal shape, we adopt a bi-variate Gaussian Mixture Model, that is capable of modelling (2D) ellipsoids

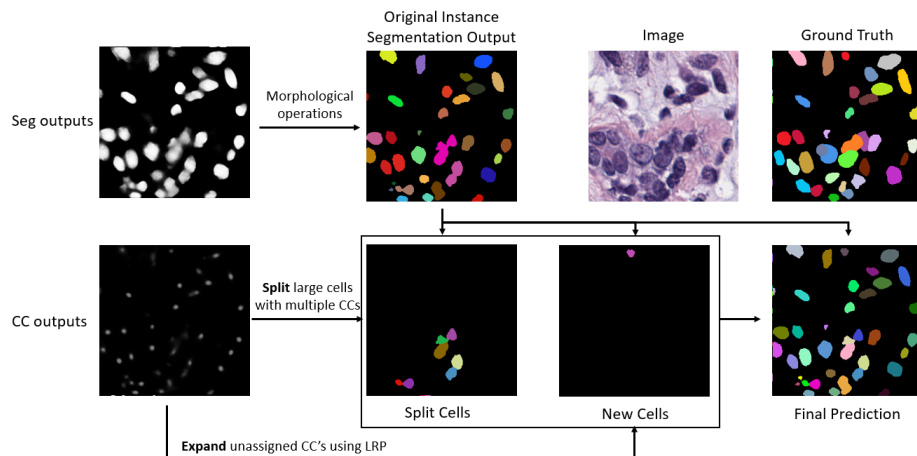


Fig. 2. An overview of our two-step procedure of Split and Expand. The Split step splits clumps of cells in the original instance segmentation output into smaller instances (e.g. the pink clump at the center is split into separate brown, green and purple instances). The Expand step “expands” unassigned CC’s using LRP into cell instances (e.g. a “new” small pink cell is shown here). We highlight that this procedure is *training-free*.

by fitting appropriate covariance values. More specifically, the algorithm will cluster all points within the clump into k (ellipsoidal) clusters, where each point is weighted by the (non-negative) CC prediction values. As such, pixels with lower CC prediction values are likelier to be points on the cell’s boundary, while pixels with higher CC prediction values are likelier to be at the center of the cell. Overall, this step can split clumps successfully into instances that match the ground truth well, as shown in Figure 2. We find this method to work well over other clustering methods or splitting based on distance metrics.

Next is the *Expand* step, which is short for CC-Expansion. We first identify CC predictions that are not contained in any instances in our original segmentation map – intuitively, these represent CC points of cells that should have been identified but were missed in the segmentation map. We next “expand” these CC points into entire cell instances. Using a single backward pass in LRP on the identified blobs in the CC outputs, we obtain an “explanation” heatmap of the positive CC predictions, which closely resembles the shape of those cells. Intuitively, this is because each positive CC prediction should be explained by the presence of a cell instance around it (which is materialized using LRP). After applying a heatmap threshold, we obtain the instance segmentation map of these cells. We note that this method is *efficient* as *only one LRP backward pass is needed per input sample*. Furthermore, in order to prevent repeat cells or generating new clumps of cells, an overlap threshold ($\frac{|Cell_1 \cap Cell_2|}{\min(|Cell_1|, |Cell_2|)}$) is implemented to discard instances with large overlaps with any existing cells.

A Split & Expand algorithm summary can be found in the Supplementary.

4 Experiment details

We experiment using two baseline methods [20,10] that use different models, losses and coarse labels (for training the segmentation head). We duplicate the last two layers of both baseline models to form the CC output branch.

Each model was trained for 150 epochs using an Adam optimizer with a learning rate of 0.001. We set $\alpha_P = 0.5, \alpha_{FRW} = 0.5$ when L_{FRW} is used, otherwise $\alpha_P = 1.0$. The FRW loss is computed using the feature map at the first encoding layer. We set our small object threshold at 10, CC confidence threshold at 0.05, heatmap threshold at 0.1 and overlap threshold at 0.5. Images were augmented using random resizing, rotations, flips, crops and affine transformations.

Following the experimental set-up of [10,26,29], we evaluated our methods on two publicly available datasets: the MoNuSeg (Multi-Organ Nucleus Segmentation) dataset [15] and the TNBC (Triple Negative Breast Cancer) dataset [17]. MoNuSeg contains 30 fully-annotated 1000x1000 H&E stained histology images of different organs. TNBC contains 50 fully-annotated 512x512 H&E stained histology images from different parts of tissue of patients with the same cancer type. Following the procedure of [10,26,29], we perform 10-fold cross-validation on both of them, taking the ratio of training:validation:test to be 8:1:1.

5 Results and Discussion

In our experiments, we report 4 metrics: AJI, object-level DICE, small-cell AJI and small-cell DICE. **AJI** is a Jaccard overlap between the set of ground truths and segmented instances, calculated across the pairwise union and intersection between each ground truth and its assigned “best” instance. **Object-level DICE** (DICE) is a weighted sum of pixel-wise F1 scores between each ground truth cell and the best assigned segmented instance, as well as between each segmented instance and the best assigned ground truth cell, *weighted by the size of the cell or instance*. Both AJI and DICE are important metrics adopted in previous works to measure instance segmentation quality [20,26,8], and can take values between 0 (worst) and 1 (best). However, these metrics are more affected by large cells compared to small cells, and *small instances only minimally affect them*, which means that they are inadequate to fairly quantify the improvements from our Expand step (where large cells are generally untouched). Thus, we report two new metrics: **small-cell AJI** and **small-cell DICE**, which are equivalent to AJI and DICE applied on small cells only. Specifically, we define a pixel size threshold (which we set to 300), and only compute the metrics for ground truth cells or segmented instances with sizes below that threshold.

We report our experiment results on the MoNuSeg in Table 1 and TNBC in Table 5. The **Baseline** setting refers to our implementation of the segmentation baselines in [20] and [10], the **Split** setting refers to the scenario where we only apply the *Split* procedure on the segmentation baseline, and **Split & Expand** refers to our full method. We also compute the statistical significance (at 0.05 significance) of our improvements by performing a paired t-test between (Baseline and Split) and (Split and Split & Expand)

Table 1. Split and Expand results on MoNuSeg (Top) and TNBC (Bottom) datasets. Best results are in bold. On all settings and metrics, our full Split and Expand method obtains significant improvements over the baseline method. Our Split step consistently provides significant improvements on the AJI and DICE metrics, while our Expand step consistently provides significant improvements on the small-cell metrics.

| Methods | Configuration | AJI | DICE | AJI (small) | DICE (small) |
|------------|----------------|----------------|--------------|----------------|----------------|
| Weakly[20] | Baseline | 0.488 | 0.692 | 0.206 | 0.384 |
| | Split | 0.512* | 0.708* | 0.209 | 0.391* |
| | Split & Expand | 0.524** | 0.710 | 0.221** | 0.409** |
| MaskGA[10] | Baseline | 0.482 | 0.705 | 0.196 | 0.379 |
| | Split | 0.534* | 0.728* | 0.214* | 0.402* |
| | Split & Expand | 0.551** | 0.732 | 0.228** | 0.417** |
| Weakly[20] | Baseline | 0.516 | 0.698 | 0.199 | 0.372 |
| | Split | 0.528* | 0.706* | 0.203* | 0.377 |
| | Split & Expand | 0.531 | 0.707 | 0.215** | 0.387** |
| MaskGA[10] | Baseline | 0.505 | 0.707 | 0.190 | 0.395 |
| | Split | 0.532* | 0.720* | 0.204* | 0.406* |
| | Split & Expand | 0.533 | 0.721 | 0.216** | 0.418** |

* significant results from paired t-test between Baseline and Split

** significant results from paired t-test between Split and Split & Expand

Overall, our full *Split* and *Expand* method produces substantial gains **over all metrics and all settings**. It is worthwhile to note that this is achieved without explicit training in our *Split* and *Expand* method.

Specifically, the Split step provides a significant improvement in object-level DICE and AJI in **all settings (highlighted in blue)**, demonstrating its effectiveness in splitting clumps of cell instances. We emphasize to the reader that this significant improvement comes from splitting clumps only, *without changing the segmentation map*. Qualitative validation is provided in the Supplementary.

Next, we observe that the Expand step improves small-cell AJI and DICE significantly in **all settings (highlighted in green)**, which validates its efficacy in identifying cells missed in the segmentation map. Although the improvement of the Expand step on AJI and object-level DICE is not very significant, this is to be expected, as the Expand step targets small cells, which have minimal impact on those metrics. Qualitative visualization is provided in the Supplementary.

Table 2. Evaluation of FRW loss on MoNuSeg dataset. Best results are in bold.

| Methods | Configuration | AJI | DICE | AJI (small) | DICE (small) |
|------------|---------------|--------------|--------------|--------------|--------------|
| Weakly[20] | Without FRW | 0.518 | 0.706 | 0.219 | 0.399 |
| | With FRW | 0.524 | 0.710 | 0.221 | 0.409 |
| MaskGA[10] | Without FRW | 0.538 | 0.728 | 0.217 | 0.411 |
| | With FRW | 0.551 | 0.732 | 0.228 | 0.417 |

Lastly, we evaluate the impact of the FRW loss in Table 2 and find that it provides consistent improvements over all metrics, which shows its effectiveness.

6 Conclusion

This paper proposes a novel two-step inference-time method (*Split* and *Expand*) for weakly supervised cell instance segmentation that is *training-free* and can be *easily applied* to many existing baseline segmentation models. A novel FRW loss based on explanation methods is also proposed to help improve cell-center predictions. We test the method on MoNuSeg and TNBC datasets, observing significant object-level improvements.

References

1. Anders, C.J., Marinč, T., Neumann, D., Samek, W., Müller, K.R., Lapuschkin, S.: Analyzing imagenet with spectral relevance analysis: Towards imagenet un-hans’ ed. arXiv preprint arXiv:1912.11425 (2019)
2. Arras, L., Montavon, G., Müller, K.R., Samek, W.: Explaining recurrent neural network predictions in sentiment analysis. In: Proceedings of the 8th Workshop on Computational Approaches to Subjectivity, Sentiment and Social Media Analysis. pp. 159–168 (2017)
3. Arras, L., Osman, A., Müller, K.R., Samek, W.: Evaluating Recurrent Neural Network Explanations. In: Proceedings of the ACL 2019 BlackboxNLP Workshop on Analyzing and Interpreting Neural Networks for NLP. pp. 113–126. ACL (2019)
4. Bach, S., Binder, A., Montavon, G., Klauschen, F., Müller, K.R., Samek, W.: On pixel-wise explanations for non-linear classifier decisions by layer-wise relevance propagation. PLOS ONE **10**(7), e0130140 (2015)
5. Bearman, A., Russakovsky, O., Ferrari, V., Fei-Fei, L.: What’s the point: Semantic segmentation with point supervision. In: European conference on computer vision. pp. 549–565. Springer (2016)
6. Beck, A.H., Sangoi, A.R., Leung, S., Marinelli, R.J., Nielsen, T.O., van de Vijver, M., West, R.B., van de Rijn, M., Koller, D.: Systematic analysis of breast cancer morphology uncovers stromal features associated with survival. Science Translational Medicine **3**, 108ra113 – 108ra113 (2011)
7. Boutros, M., Heigwer, F., Laufer, C.: Microscopy-based high-content screening. Cell **163**(6), 1314 – 1325 (2015)
8. Chamanzar, A., Nie, Y.: Weakly supervised multi-task learning for cell detection and segmentation. In: 2020 IEEE 17th ISBI. pp. 513–516. IEEE (2020)
9. Filipczuk, P., Fevens, T., Krzyżak, A., Monczak, R.: Computer-aided breast cancer diagnosis based on the analysis of cytological images of fine needle biopsies. IEEE T-MI **32**(12), 2169–2178 (2013)
10. Guo, R., Pagnucco, M., Song, Y.: Learning with noise: Mask-guided attention model for weakly supervised nuclei segmentation. In: International Conference on Medical Image Computing and Computer-Assisted Intervention. pp. 461–470. Springer (2021)
11. Halliwell, N., Lecue, F.: Trustworthy convolutional neural networks: A gradient penalized-based approach. arXiv preprint arXiv:2009.14260 (2020)
12. Hesamian, M.H., Jia, W., He, X., Kennedy, P.: Deep learning techniques for medical image segmentation: Achievements and challenges. Journal of digital imaging **32**(4), 582–596 (August 2019)
13. Kauffmann, J., Esders, M., Montavon, G., Samek, W., Müller, K.R.: From clustering to cluster explanations via neural networks. arXiv:1906.07633 (2019)

14. Kohlbrenner, M., Bauer, A., Nakajima, S., Binder, A., Samek, W., Lapuschkin, S.: Towards best practice in explaining neural network decisions with LRP. In: IJCNN. pp. 1–7 (2020)
15. Kumar, N., Verma, R., Sharma, S., Bhargava, S., Vahadane, A., Sethi, A.: A dataset and a technique for generalized nuclear segmentation for computational pathology. *IEEE T-MI* **36**(7), 1550–1560 (2017)
16. Lapuschkin, S., Wäldchen, S., Binder, A., Montavon, G., Samek, W., Müller, K.R.: Unmasking clever hans predictors and assessing what machines really learn. *Nature Communications* **10**(1), 1096 (2019)
17. Naylor, P., Laé, M., Reyat, F., Walter, T.: Segmentation of nuclei in histopathology images by deep regression of the distance map. *IEEE T-MI* **38**(2), 448–459 (2019)
18. Obikane, S., Aoki, Y.: Weakly supervised domain adaptation with point supervision in histopathological image segmentation. In: Cree, M., Huang, F., Yuan, J., Yan, W.Q. (eds.) *Pattern Recognition*. pp. 127–140. Springer Singapore, Singapore (2020)
19. Poerner, N., Roth, B., Schütze, H.: Evaluating neural network explanation methods using hybrid documents and morphosyntactic agreement. In: *Proceedings of the 56th ACL (Volume 1: Long Papers)*. p. 340–350. ACL (2018)
20. Qu, H., Wu, P., Huang, Q., Yi, J., Riedlinger, G.M., De, S., Metaxas, D.N.: Weakly supervised deep nuclei segmentation using points annotation in histopathology images. In: *International Conference on Medical Imaging with Deep Learning*. pp. 390–400 (2019)
21. Qu, H., Wu, P., Huang, Q., Yi, J., Yan, Z., Li, K., Riedlinger, G.M., De, S., Zhang, S., Metaxas, D.N.: Weakly supervised deep nuclei segmentation using partial points annotation in histopathology images. *IEEE T-MI* **39**(11), 3655–3666 (Nov 2020)
22. Samek, W., Binder, A., Montavon, G., Lapuschkin, S., Müller, K.R.: Evaluating the visualization of what a deep neural network has learned. *IEEE TNNLS* **28**(11), 2660–2673 (2016)
23. Schnake, T., Eberle, O., Lederer, J., Nakajima, S., Schütt, K.T., Müller, K.R., Montavon, G.: XAI for Graphs: Explaining graph neural network predictions by identifying relevant walks. *arXiv preprint arXiv:2006.03589* (2020)
24. Sun, J., Lapuschkin, S., Samek, W., Binder, A.: Understanding image captioning models beyond visualizing attention. *arXiv preprint arXiv:2001.01037* (2020)
25. Sun, J., Lapuschkin, S., Samek, W., Zhao, Y., Cheung, N.M., Binder, A.: Explanation-guided training for cross-domain few-shot classification. In: *2020 25th International Conference on Pattern Recognition (ICPR)*. pp. 7609–7616. IEEE (2021)
26. Tian, K., Zhang, J., Shen, H., Yan, K., Dong, P., Yao, J., Che, S., Luo, P., Han, X.: Weakly-supervised nucleus segmentation based on point annotations: A coarse-to-fine self-stimulated learning strategy. In: Martel, A.L., Abolmaesumi, P., Stoyanov, D., Mateus, D., Zuluaga, M.A., Zhou, S.K., Racoceanu, D., Joskowicz, L. (eds.) *MICCAI 2020*. pp. 299–308. Springer International Publishing, Cham (2020)
27. Ulman, V., Maška, M., Magnusson, K., Ronneberger, O., Haubold, C., Harder, N., Matula, P., Matula, P., Svoboda, D., Radojevic, M., Smal, I., Rohr, K., Jaldén, J., Blau, H., Dzyubachyk, O., Lelieveldt, B., Xiao, P., Li, Y., Cho, S.Y., Ortiz-de Solorzano, C.: An objective comparison of cell tracking algorithms. *Nature Methods* **14** (12 2017)
28. Yen, T.A., Hsu, H.C., Pati, P., Gabrani, M., Foncubierta-Rodríguez, A., Chung, P.C.: Ninepins: Nuclei instance segmentation with point annotations. *arXiv preprint arXiv:2006.13556* (2020)

29. Yoo, I., Yoo, D., Paeng, K.: Pseudoedgenet: Nuclei segmentation only with point annotations. In: MICCAI. pp. 731–739. Springer (2019)